Finite Time Identical Synchronization in Networks with Arbitrary Topological Structures of n Coupled Dynamical Systems of the Hindmarsh-Rose 3D Type

Phan Van Long Em

***Abstract*—In this work, an adaptive nonlinear control scheme is developed to achieve finite-time identical synchronization in complex networks with arbitrary topology, comprising n interconnected nodes. The dynamics of each node are governed by the three-dimensional Hindmarsh-Rose model. Theoretical results are corroborated through numerical simulations implemented in R, illustrating the effectiveness and robustness of the proposed synchronization approach.**

***Index Terms*—controller, finite time identical synchronization, Hindmarsh-Rose 3D model, networks with arbitrary structure.**

I. Introduction

THE phenomenon of synchronization, wherein multiple interacting systems spontaneously coordinate their dynamics, has emerged as a fundamental topic in nonlinear science. From biological rhythms and chemical oscillations to power grid dynamics and communication networks, synchronization is a pervasive feature of both natural and artificial systems [1], [3], [4], [5], [6], [7], [8]. At its core, synchronization entails the adjustment of rhythms or states of oscillatory systems through coupling or mutual interaction, often leading to coherent behavior across complex networked systems. This intrinsic capacity for coherence, even in the presence of heterogeneous individual dynamics and intricate interconnections, has inspired extensive theoretical and empirical investigations across disciplines.

Over the past few decades, the study of synchronization has evolved from simple pairwise oscillator models to large-scale, complex dynamical networks. This transition has been motivated by the increasing need to understand and control systems composed of numerous interconnected components. Examples include neural networks in the brain, gene regulatory networks, ecological food webs, social interaction networks, and engineered infrastructures such as the Internet and smart grids [21], [22], [23], [24]. These systems typically exhibit nonlinear interactions, varying connection strengths, and dynamic topologies, making the study of their collective behavior both challenging and essential.

Within this broad framework, complex dynamical networks have garnered particular attention. Such networks are composed of nodeseach representing an individual dynamical systemand edges that define the interaction rules among them. Understanding how these coupled systems synchronize provides valuable insights into global behaviors emerging from local interactions. Moreover, it paves the way for developing control strategies in applications ranging from secure communication and pattern recognition to disease modeling and brain-machine interfaces.

A significant body of research has focused on asymptotic synchronization, where networked systems gradually converge to a common trajectory as time progresses toward infinity. While asymptotic results offer theoretical insight into long-term behavior, they are often insufficient in practical contexts where convergence within finite time is critical. For instance, rapid coordination is vital in power systems to avoid cascading failures, in robotics for real-time task execution, or in neural systems for cognitive processing. Consequently, finite-time synchronization-achieving identical synchronization within a finite interval-has become an active area of research [10], [11], [1], [14], [15], [17].

Finite-time synchronization brings forth several advantages over its asymptotic counterpart. Chief among them is the possibility of establishing explicit bounds on convergence time, which is essential for real-time control and performance guarantees in engineering systems. Additionally, finite-time control strategies often exhibit greater robustness to perturbations, modeling uncertainties, and time-varying disturbances. Despite these advantages, developing systematic methods for finite-time synchronization remains nontrivial due to the inherently nonlinear and discontinuous nature of the underlying control laws.

Compounding this challenge is the fact that most theoretical studies to date have focused on networks with highly idealized structures, such as globally coupled systems, hierarchical trees, or regular chains [14], [15], [17], [10]. While these models are mathematically tractable, they rarely capture the complexity of real-world networks, which often exhibit arbitrary, heterogeneous, or even evolving topologies. Real neural networks, for instance, are known to display small-world and scale-free properties, with nonuniform connectivity and diverse nodal dynamics. Hence, extending finite-time synchronization theory to networks with arbitrary topology is of both theoretical significance and practical relevance.

Motivated by these considerations, the present work seeks to address a critical gap in the literature by investigating finite-time identical synchronization in networks of Hindmarsh-Rose (HR) neurons with arbitrary coupling topology. The HR model, a three-dimensional system of nonlinear differential equations, captures a wide range of neuronal

Manuscript received June 16, 2025; revised August 15, 2025.

Phan Van Long Em is a lecturer of An Giang University, Vietnam National University, Ho Chi Minh City, VIETNAM (e-mail: pvlem@agu.edu.vn).

behaviors, including bursting, spiking, and chaotic dynamics [2]. Due to its biological relevance and mathematical richness, the HR model is widely used in computational neuroscience and nonlinear dynamics. In this study, each node of the network is represented by a Hindmarsh-Rose oscillator, and interactions among nodes are modeled through linear coupling governed by an arbitrary Laplacian matrix.

The main objective of this paper is to derive sufficient conditions under which a network of n linearly coupled HR neurons achieves identical synchronization in finite time. That is, despite potential differences in initial conditions and network structure, all nodes in the network converge to a common trajectory within a guaranteed time bound. To this end, we employ tools from finite-time stability theory, particularly the use of Lyapunov functions with negative definite fractional powers, which are instrumental in establishing finite-time convergence results.

Our approach involves the design of a distributed control law that is both scalable and implementable in decentralized settings. This control law is constructed based on the differences in states between connected nodes and includes a nonlinear damping term to enforce finite-time convergence. We further construct a composite Lyapunov function that accounts for the network topology, nodal dynamics, and coupling interactions. Through rigorous analysis, we derive an explicit upper bound on the synchronization time and provide constructive criteria that ensure global finite-time synchronization of the network.

To validate the theoretical findings, we conduct numerical simulations on networks with varying topologies. The simulation results demonstrate that the proposed control scheme achieves fast and robust synchronization, even under structural complexity and parameter heterogeneity. The results highlight the practicality and effectiveness of our approach in capturing realistic network behaviors.

The contributions of this paper are threefold: We extend the theory of finite-time synchronization to networks with arbitrary topology, moving beyond the limitations of previous studies restricted to symmetric or structured graphs; We establish a general theoretical framework for finite-time identical synchronization in coupled Hindmarsh-Rose neural systems using nonlinear control techniques and Lyapunov-based analysis; We provide robust numerical evidence supporting the analytical results, thereby demonstrating the potential applicability of our methods in modeling and control of complex biological and engineering networks.

The remainder of the paper is organized as follows. In Section 2, we formulate the network model, introduce relevant mathematical preliminaries, and present the main synchronization results. Section 3 contains numerical experiments that illustrate the performance of the proposed synchronization scheme under various network conditions. Finally, Section 4 concludes the paper with a summary of findings and suggestions for future research directions.

II. Finite time identical synchronization in the networks with arbitrary topological struture of n coupled dynamical systems of the Hindmarsh-Rose 3D type

In their seminal 1952 work, A. L. Hodgkin and A. F. Huxley developed a biophysically grounded model that captured the dynamic behavior of the neuronal membrane potential through a system of four coupled ordinary differential equations (ODEs) [4], [2], [7]. This pioneering model represented a major advancement in theoretical neuroscience, as it provided a quantitative framework for describing the ionic mechanisms underlying action potential generation and propagation in neurons. The mathematical rigor and physiological accuracy of the Hodgkin-Huxley model earned the authors the Nobel Prize, and their formulation has since served as a cornerstone in the modeling of excitable biological membranes.

In the decades following their publication, significant effort has been directed toward simplifying the original Hodgkin-Huxley system while preserving its essential dynamical and energetic characteristics. Among the more influential simplifications is the model introduced by J. L. Hindmarsh and R. M. Rose in 1984 [9], [7]. This model reduces the dimensionality of the original system to three coupled ODEs, making it more tractable for both analytical and numerical investigation. Despite its reduced complexity, the Hindmarsh-Rose model retains the ability to replicate key features of neuronal activity, including bursting, spiking, and chaotic dynamics [6].

The state variables in the Hindmarsh-Rose model are denoted by u, v, and w. The variable u represents the membrane potential, while v and w correspond to recovery variables associated with the fast and slow currents across the membrane, respectively. These auxiliary variables are typically interpreted in terms of ionic conductances and gating mechanisms, albeit in a phenomenological rather than biophysical manner. The reduced dimensionality and simplified structure of the Hindmarsh-Rose model make it particularly suitable for theoretical analysis and large-scale network simulations, where computational efficiency is critical.

The system of equations describing the Hindmarsh-Rose 3D model is given by the following set of ordinary differential equations [9], [2], [7]:

$$\begin{cases} \dfrac{du}{dt} = u_t = f(u) + v - w + I, \\ \dfrac{dv}{dt} = v_t = 1 - bu^2 - v, \\ \dfrac{dw}{dt} = w_t = r(s(u - c) - w), \end{cases} \tag{1}$$

where $u = u(t), v = v(t), w = w(t)$; $f(u) = -u^3 + au^2$; a, b, c, r, s are constants $(a, b, r, s > 0)$; I presents the external current; t presents the time. These equations form a rich dynamical system capable of emulating a wide spectrum of electrophysiological phenomena observed in real neurons.

In the following analysis, the dynamical system described by Equation (1) is interpreted as a neural model. A network comprising n linearly coupled instances of this system is then constructed, as given by:

$$\begin{cases} u_{it} = f(u_i) + v_i - w_i + I + \sum\limits_{j=1, j\neq i}^{n} c_{ij} h(u_i, u_j), \\ v_{it} = 1 - bu_i^2 - v_i, \\ w_{it} = r(s(u_i - c) - w_i), \\ i = 1, 2, ..., n, \end{cases} \tag{2}$$

where $(u_i, v_i, w_i), i = 1, 2, ..., n$, is defined as in (1); The coefficients c_{ij} are the elements of the connectivity matrix $C_n = (c_{ij})_{n\times n}$, defined by: $c_{ij} > 0$ if neuron ith and jth are coupled, $c_{ij} = 0$ if neuron ith and jth are not coupled, and $c_{ii} = -\sum_{j\neq i, j=1}^{n} c_{ij}$, where $i, j = 1, 2, ..., n, i \neq j$. This matrix also illustrates the network topology. The function h describes the coupling between the i-th and j-th cells. As is well known, neurons communicate through synapses, resulting in two primary types of connections: chemical and electrical. Mathematically, when neurons are connected via chemical synapses, the coupling function is nonlinear [10], [11], [2]. It is expressed by the following formula:

$$\begin{cases} h(u_i, u_j) = -g_{syn}(u_i - V_{syn})\dfrac{1}{1+\exp(-\lambda(u_j - \theta_{syn}))}, \\ i = 1, 2, ..., n, \end{cases} \tag{3}$$

In this context, let u_j for $j = 1, 2, \ldots, n$ represent the j-th node connected to the i-th node. The coupling strength is denoted by g_{syn}, which is a positive number. The reversal potential, V_{syn}, must be greater than $u_i(x, t)$ for all $i = 1, 2, \ldots, n$, as well as for any $x \in \Omega$ and $t \geq 0$. This is because the synapses are assumed to be excitatory. Additionally, θ_{syn} is the threshold that must be reached by each action potential for a neuron. The parameter λ is also a positive number. The larger the value of λ, the closer we approach the Heaviside function.

If neurons connect through electrical synapses, the coupling function is linear [2], [14] and is expressed by the following formula:

$$h(u_i, u_j) = -g_{syn}(u_i - u_j),\ i, j = 1, 2, ..., n, \tag{4}$$

where g_{syn} is positive number presenting the coupling strength.

In this study, we propose an adaptive nonlinear controller designed to achieve finite-time identical synchronization of the network described by equation (2). Prior to the development of the controller, several important remarks and lemmas are reviewed to support the subsequent analysis.

Remark 1 (see [17])**.** The function f satisfies the following condition:

$$|f(u_i) - f(u_j)| \leq \alpha\,|u_i - u_j|\,, \tag{5}$$

where $u_i, u_j, i, j = 1, 2, ..., n$, present the transmembrane voltages, and α is a positive number.

Remark 2 (see [17])**.** The function h defined by (3) and (4) satisfies the following condition:

$$\begin{cases} |h(u_i, u_k) - h(u_j, u_l)| \leq \beta\,|u_i - u_j|\,, \\ i, j, k, l = 1, 2, ..., n, i \neq k, j \neq l, \end{cases} \tag{6}$$

where u_i, u_j, u_k, u_l present the transmembrane voltages, and β is a positive number.

Lemma 1 ([19])**.** *For every $a_i \in \mathbb{R}, i = 1, 2, ..., n$, if $p, q \in \mathbb{R}, 0 < p \leq 1, 0 < q < 2$, then we have:*

$$\sum_{i=1}^{n} |a_i|^q \geq \left(\sum_{i=1}^{n} |a_i|^2\right)^{\frac{q}{2}} \text{ and } \left(\sum_{i=1}^{n} |a_i|\right)^p \leq \sum_{i=1}^{n} |a_i|^p.$$

Lemma 2 ([20])**.** *Assume that a continuous, positive-definite function $V(t)$ satisfies the following differential inequality:*

$$\frac{dV(t)}{dt} \leq -\epsilon V^{\mu}(t),\ \textit{for all } t \geq 0, V(0) \geq 0,$$

where μ, ϵ are positive constants and $0 < \mu < 1$, then

$$\begin{cases} V^{1-\mu}(t) \leq V^{1-\mu}(0) - \epsilon(1-\mu)t, \quad 0 < t < t^*, \\ V(t) \equiv 0,\ \ t > t^* = \dfrac{V^{1-\mu}(0)}{\epsilon(1-\mu)}, \end{cases}$$

Let the node errors of identical synchronization of the network (2) be $e_i^u = u_i - u_1, e_i^v = v_i - v_1, e_i^w = w_i - w_1$, for all $i = 2, ..., n$. The finite time identical synchronization problem of the network (2) can be defined as follows:

Definition 1. If there is a time $t^* > 0$ such that:

$$\lim_{t\to t^*} \sum_{i=2}^{n} (|e_i^u| + |e_i^v| + |e_i^w|) = 0,$$

and

$$\sum_{i=2}^{n} (|e_i^u| + |e_i^v| + |e_i^w|) \equiv 0,\ \text{for all } t > t^*,$$

where t^* is called the setting time, then the full network (2) is synchrous in a finite time.

To get the identical synchronization in a finite time, we need to define the controllers for the network (2) by constructing and adding the controllers into neuron ith, $i \neq 1$, as follows:

$$\begin{cases} u_{1t} = f(u_1) + v_1 - w_1 + I + \sum_{j=2}^{n} c_{1j} h(u_1, u_j) \\ v_{1t} = 1 - bu_1^2 - v_1, \\ w_{1t} = r(s(u_1 - c) - w_1), \\ u_{it} = f(u_i) + v_i - w_i + I + \sum_{j=1, j\neq i}^{n} c_{ij} h(u_i, u_j) + \Gamma_i^1, \\ v_{it} = 1 - bu_i^2 - v_i + \Gamma_i^2, \\ w_{it} = r(s(u_i - c) - w_i) + \Gamma_i^3, \\ i = 2, ..., n, \end{cases} \tag{7}$$

where the controllers $\Gamma_i^j = \Gamma_i^j(t), i = 2, 3, ..., n; j = 1, 2, 3$, will be designed as follows:

$$\begin{cases} \Gamma_i^1 = u_{1t} - f(u_1) - v_1 + w_1 - I \\ \qquad - \sum_{j=1, j\neq i}^{n} c_{ij} h(u_1, u_j) - k_i e_i^u + G_i^1, \\ \Gamma_i^2 = v_{1t} - 1 + bu_1^2 + v_1 + G_i^2, \\ \Gamma_i^3 = w_{1t} - r(s(u_1 - c) - w_1) + G_i^3, \end{cases} \tag{8}$$

with the updated rules defined as follows:

$$k_{it} = r_i((e_i^u)^2 + \theta_i), \tag{9}$$

where $k_i = k_i(t)$; r_i is a arbitrary positive constant, for $i = 2, ..., n$, and $G_i^j = G_i^j(t), \theta_i = \theta_i(t), j = 1, 2, 3; i = 2, 3, ..., n$, are defined as follows:

$$\begin{cases} G_i^1 = -m.sign(e_i^u)|e_i^u|^\gamma, \\ G_i^2 = -m.sign(e_i^v)|e_i^v|^\gamma, \\ G_i^3 = -m.rs.sign(e_i^w)|e_i^w|^\gamma, \\ \theta_i = -m.sign(k_i - k).|k_i - k|^\gamma, \end{cases} \tag{10}$$

where $sign(.)$ represents a signum function; m is a given positive constant; $\gamma \in \mathbb{R}$ and satisfies $0 \leq \gamma < 1$; and k is a positive cosntant to be determined.

Under the action of the controllers designed as above, the error dynamic equations of the system (2) are described as:

$$\begin{aligned} e_{it}^u &= (u_{it} - u_{1t}) \\ &= f(u_i) + v_i - w_i + I + \sum_{j=1,j\neq i}^{n} c_{ij}h(u_i,u_j) \\ &\quad -f(u_1) - v_1 + w_1 - I \\ &\quad - \sum_{j=1,j\neq i}^{n} c_{ij}h(u_1,u_j) - k_i e_i^u + G_i^1 \\ &= f(u_i) - f(u_1) + (v_i - v_1) - (w_i - w_1) \\ &\quad + \sum_{j=1,j\neq i}^{n} c_{ij}(h(u_i,u_j) - h(u_1,u_j)) - k_i e_i^u + G_i^1 \\ &= f(u_i) - f(u_1) + e_i^v - e_i^w \\ &\quad + \sum_{j=1,j\neq i}^{n} c_{ij}(h(u_i,u_j) - h(u_1,u_j)) - k_i e_i^u + G_i^1, \end{aligned} \tag{11}$$

$$\begin{aligned} e_{it}^v &= v_{it} - v_{1t} \\ &= 1 - bu_i^2 - v_i - 1 + bu_1^2 + v_1 + G_i^2 \\ &= -b(u_i + u_1)e_i^u - e_i^v + G_i^2, \end{aligned} \tag{12}$$

and

$$\begin{aligned} e_{it}^w &= w_{it} - w_{1t} \\ &= r(s(u_i - c) - w_i) - r(s(u_1 - c) - w_1) + G_i^3 \\ &= rs(u_i - u_1) - r(w_i - w_1) + G_i^3 \\ &= rse_i^u - re_i^w + G_i^3, \end{aligned} \tag{13}$$

for $i = 2, ..., n$.

Subsequently, employing Lyapunov function methods and finite-time stability theory, the finite-time identical synchronization problem of the complex network described by (2) is investigated. The principal result is presented in the following theorem.

Theorem 1. *The full network* (2) *can achieve identical synchronization in a finite time under the adaptive controller* (8) *and updated rule* (9)*. The setting time is estimated as:*

$$t^* = \frac{V^{\frac{1-\gamma}{2}}(0)}{m\rho^{\frac{\gamma-1}{2}}(1-\gamma)},$$

where $\rho = \min\{2, 2rs, 2r_i\}, i = 2, 3, ..., n.$

Proof: We construct the Lyapunov function as follows:

$$V(t) = \frac{1}{2}\sum_{i=2}^{n}\left((e_i^u)^2 + (e_i^v)^2 + \frac{1}{rs}(e_i^w)^2 + \frac{1}{r_i}(k_i - k)^2\right). \tag{14}$$

Calculating the time derivative of $V(t)$ along the error systems (11) - (13), we get:

$$\begin{aligned} \frac{dV(t)}{dt} &= \sum_{i=2}^{n}\left[e_i^u e_{it}^u + e_i^v e_{it}^v + \frac{1}{rs}e_i^w e_{it}^w + \frac{1}{r_i}(k_i - k)k_{it}\right] \\ &= \sum_{i=2}^{n}\Big[e_i^u\left(f(u_i) - f(u_1) + e_i^v - e_i^w\right. \\ &\quad \left. + \sum_{j=1,j\neq i}^{n} c_{ij}(h(u_i,u_j) - h(u_1,u_j)) - k_i e_i^u + G_i^1\right) \\ &\quad -b(u_i + u_1)e_i^u e_i^v - (e_i^v)^2 \\ &\quad +e_i^v G_i^2 + k_i(e_i^u)^2 - k(e_i^u)^2 + (k_i - k)\theta_i \\ &\quad \left. +\frac{1}{rs}(rse_i^u e_i^w - r(e_i^w)^2 + e_i^w G_i^3)\right] \\ &= \sum_{i=2}^{n}\Big[e_i^u\left(f(u_i) - f(u_1)\right) + e_i^u G_i^1 \\ &\quad +(1 - b(u_i + u_1))e_i^u e_i^v - k(e_i^u)^2 + e_i^v G_i^2 \\ &\quad + \sum_{j=1,j\neq i}^{n} c_{ij}(h(u_i,u_j) - h(u_1,u_j)) - (e_i^v)^2 \\ &\quad \left. +(k_i - k)\theta_i - \frac{1}{s}(e_i^w)^2 + \frac{1}{rs}e_i^w G_i^3\right]. \end{aligned} \tag{15}$$

By using Remarks 1 and 2, it is easy to obtain:

$$\begin{aligned} \frac{dV(t)}{dt} &\leq \sum_{i=2}^{n}\Bigg[\alpha(e_i^u)^2 + \sum_{j=1,j\neq i}^{n}\beta c_{ij}(e_i^u)^2 - (e_i^v)^2 \\ &\quad -\frac{1}{s}(e_i^w)^2 + e_i^u G_i^1 + e_i^v G_i^2 + \frac{1}{rs}e_i^w G_i^3 - k(e_i^u)^2 \\ &\quad +(k_i - k)\theta_i + (1 + b(|u_i| + |u_1|))|e_i^u||e_i^v|] \\ &\leq \sum_{i=2}^{n}\Bigg[\alpha(e_i^u)^2 + \beta(n-1)\max_{1\leq j\leq n, j\neq i}|c_{ij}|(e_i^u)^2 - (e_i^v)^2 \\ &\quad -\frac{1}{s}(e_i^w)^2 + e_i^u G_i^1 + e_i^v G_i^2 + \frac{1}{rs}e_i^w G_i^3 - k(e_i^u)^2 \\ &\quad +(k_i - k)\theta_i + (1 + b(|u_i| + |u_1|))|e_i^u||e_i^v|] \end{aligned} \tag{16}$$

By using the Young's inequality for every $\delta > 0$, we can see:

$$\begin{aligned} &|e_i^u|\,|e_i^v|\,(1 + b(|u_i| + |u_1|)) \\ &\quad \leq (1 + b(|u_i| + |u_1|))(\frac{1}{2\delta}(e_i^u)^2 + \frac{\delta}{2}(e_i^v)^2) \\ &\quad \leq \frac{M}{2\delta}(e_i^u)^2 + \frac{M\delta}{2}(e_i^v)^2, \end{aligned} \tag{17}$$

where M is a positive constant, since $u_i, i = 1, 2, ..., n$ are bounded (see [16]).

Combining (16) and (17) yields:

$$\frac{dV(t)}{dt} \leq \sum_{i=2}^{n}\Bigg[(\alpha - k + \beta(n-1)\max_{1\leq j\leq n, j\neq i}|c_{ij}| + \frac{M}{2\delta})(e_i^u)^2 - (1-\frac{M\delta}{2})\bar{e}_i{}^2 - \frac{1}{s}(e_i^w)^2 + (k_i-k)\theta_i + e_i^u G_i^1 + e_i^v G_i^2 + \frac{1}{rs}e_i^w G_i^3\Bigg]. \tag{18}$$

Chose $\delta > 0$ such that $1 - \frac{M\delta}{2} > 0$, and take

$$k > \alpha + \beta(n-1)\max_{1\leq j\leq n, j\neq i}|c_{ij}| + \frac{M}{2\delta}, \tag{19}$$

then (18) can be estimated as:

$$\frac{dV(t)}{dt} \leq \sum_{i=2}^{n}\left[(k_i-k)\theta_i + e_i^u G_i^1 + e_i^v G_i^2 + \frac{1}{rs}e_i^w G_i^3\right]. \tag{20}$$

Besides that, we can see:

$$\begin{aligned}\sum_{i=2}^{n}\left((k_i-k)\theta_i + e_i^u G_i^1 + e_i^v G_i^2 + \frac{1}{rs}e_i^w G_i^3\right) &= \sum_{i=2}^{n}(-m.(k_i-k)sign(k_i-k).|k_i-k|^{\gamma} - m.e_i^u sign(e_i^u)|e_i^u|^{\gamma} - m.e_i^v sign(e_i^v)|e_i^v|^{\gamma} - m.e_i^w sign(e_i^w)|e_i^w|^{\gamma}) \\ &\leq \sum_{i=2}^{n}\Big(-m(|k_i-k|^{\gamma+1} + |e_i^u|^{\gamma+1} + |e_i^v|^{\gamma+1} + |e_i^w|^{\gamma+1})\Big).\end{aligned} \tag{21}$$

Combining (20) - (21) yields:

$$\frac{dV(t)}{dt} \leq -m\sum_{i=2}^{n}\Big(|k_i-k|^{\gamma+1} + |e_i^u|^{\gamma+1} + |e_i^v|^{\gamma+1} + |e_i^w|^{\gamma+1}\Big). \tag{22}$$

By using Lemma 1, we have:

$$\left(\sum_{i=2}^{n}\Big(|k_i-k|^{\gamma+1} + |e_i^u|^{\gamma+1} + |e_i^v|^{\gamma+1} + |e_i^w|^{\gamma+1}\Big)\right)^{\frac{1}{\gamma+1}} \geq \left(\sum_{i=2}^{n}\Big(|k_i-k|^2 + |e_i^u|^2 + |e_i^v|^2 + |e_i^w|^2\Big)\right)^{\frac{1}{2}}. \tag{23}$$

That yields:

$$\sum_{i=2}^{n}\Big(|k_i-k|^{\gamma+1} + |e_i^u|^{\gamma+1} + |e_i^v|^{\gamma+1} + |e_i^w|^{\gamma+1}\Big) \geq \left(\sum_{i=2}^{n}\Big(|k_i-k|^2 + |e_i^u|^2 + |e_i^v|^2 + |e_i^w|^2\Big)\right)^{\frac{\gamma+1}{2}}. \tag{24}$$

Therefore, (22) becomes:

$$\begin{aligned}\frac{dV(t)}{dt} &\leq -m\left(\sum_{i=2}^{n}\Big(|k_i-k|^2 + |e_i^u|^2 + |e_i^v|^2 + |e_i^w|^2\Big)\right)^{\frac{\gamma+1}{2}} \\ &\leq -m\rho^{\frac{\gamma+1}{2}}\left(\sum_{i=2}^{n}\frac{1}{2}\left(|e_i^u|^2 + |e_i^v|^2 + \frac{1}{rs}|e_i^w|^2 + \frac{1}{r_i}|k_i-k|^2\right)\right)^{\frac{\gamma+1}{2}} \\ &\leq -m\rho^{\frac{\gamma+1}{2}}V^{\frac{\gamma+1}{2}}(t).\end{aligned} \tag{25}$$

where $\rho = \min\{2, 2rs, 2r_i\}, i = 2, 3, ..., n$.

It is derived from Lemma 2 that $V(t) \equiv 0$ for

$$t > t^* = \frac{V^{\frac{1-\gamma}{2}}(0)}{m\rho^{\frac{\gamma-1}{2}}(1-\gamma)}.$$

Therefore,

$$\lim_{t\to t^*}\sum_{i=2}^{n}(|e_i^u| + |e_i^v| + |e_i^w|) = 0,$$

and

$$\sum_{i=2}^{n}(|e_i| + |e_i| + |e_i^w|) \equiv 0 \text{ for } t > t^*.$$

This completes the proof. ■

III. Numerical results and discussion

This section evaluates the performance of the previously developed controllers. System integration was implemented using the R programming language. Simulation results were generated based on the following parameter values:

$$f(u) = -u^3 + au^2, a = 3, b = 5, s = 4, r = 0.008,$$
$$c = -\frac{1}{2}(1+\sqrt{5}), I = 3.25.$$
$$\lambda = 10,\ V_{syn} = 2,\ \theta_{syn} = -0,25.$$

Remark 3. This section is dedicated to evaluating the practical applicability of the theoretical framework developed earlier, with a specific focus on synchronization dynamics in complex networks. Unlike previous works [14], [15], which primarily establish that identical synchronization can be achieved given sufficiently large coupling strengths, the present study does not aim to pinpoint the precise coupling thresholds. Instead, it addresses a critical gap observed in the literature: theoretical analyses often conclude that synchronization is asymptotic, occurring only as time approaches infinity. In contrast, numerical simulations consistently demonstrate that identical synchronization can be realized within a finite time interval. This divergence between theory and simulation remains an unresolved issue. To bridge this gap, we propose a novel nonlinear control strategy designed to induce finite-time identical synchronization across networked systems. The theoretical foundations supporting the efficacy of this controller have been rigorously established, providing guarantees for synchronization within a finite temporal horizon. The current section seeks to validate these theoretical predictions through comprehensive numerical simulations, thereby confirming the controllers effectiveness under practical conditions. This approach not only enhances the

understanding of synchronization phenomena but also offers a viable method for implementing finite-time synchronization in real-world networked systems.

A. Example 1.

This example investigates a chain network comprising two nonlinearly coupled nodes. The objective is to design controllers, based on the theoretical framework detailed in equations (8) through (10), to achieve finite-time identical synchronization. To validate the effectiveness of the proposed control strategy, numerical simulations are conducted. The controlled system modeling the chain network with two nonlinear coupled nodes for synchronization is described as follows:

$$\begin{cases} u_{1t} = f(u_1) + v_1 - w_1 + I, \\ v_{1t} = 1 - bu_1^2 - v_1, \\ w_{1t} = r(s(u_1 - c) - w_1), \\ u_{2t} = f(u_2) + v_2 - w_2 + I \\ \quad -g_{syn}(u_2 - V_{syn})\dfrac{1}{1+\exp(-\lambda(u_1 - \theta_{syn}))} + \Gamma_2^1, \\ v_{2t} = 1 - bu_2^2 - v_2 + \Gamma_2^2, \\ w_{2t} = r(s(u_2 - c) - w_2) + \Gamma_2^3. \end{cases} \tag{26}$$

where

$$\begin{cases} \Gamma_2^1 = u_{1t} - f(u_1) - v_1 + w_1 - I - k_2 e_2^u + G_2^1 \\ \quad +g_{syn}(u_1 - V_{syn})\dfrac{1}{1+\exp(-\lambda(u_1 - \theta_{syn}))}, \\ \Gamma_2^2 = v_{1t} - 1 + bu_1^2 + v_1 + G_2^2, \\ \Gamma_2^3 = w_{1t} - r(s(u_1 - c) - w_1) + G_2^3, \end{cases} \tag{27}$$

with the updated rules defined as follows:

$$k_{2t} = r_2((e_2^u)^2 + \theta_2), \tag{28}$$

where $k_2 = k_2(t)$; r_2 is a arbitrary positive constant; $e_2^u = u_2 - u_1, e_2^v = v_2 - v_1, e_2^w = w_2 - w_1$; and $G_2^j = G_2^j(t), \theta_2 = \theta_2(t), j = 1, 2, 3$, are defined as follows:

$$\begin{cases} G_2^1 = -m.sign(e_2^u)|e_2^u|^\gamma, \\ G_2^2 = -m.sign(e_2^v)|e_2^v|^\gamma, \\ G_2^3 = -m.rs.sign(e_2^w)|e_2^w|^\gamma, \\ \theta_2 = -m.sign(k_2 - k).|k_2 - k|^\gamma, \end{cases} \tag{29}$$

where $sign(.)$ represents a signum function, m is a given positive constant, $\gamma \in \mathbb{R}$ and satisfies $0 \leq \gamma < 1$.

In this example, we take:

$$m = 0.65;\ \gamma = 0.65; r_2 = 0.002.$$

In addition, from (19), to ensure that the controller is effective, we need to choose the value of k large enough. Here, we take $k = 5$.

Let $|e_2^u| + |e_2^v| + |e_2^w|$ be the identical synchronization error. We say that the network (26) identically synchronizes in a finte time if the identical synchronization error reaches zero as t approaches a finite value. Here, we take the initial condition for the system (26) as follows:

$$(u_1(0), v_1(0), u_2(0), v_2(0)) = (0.5, 0.5, 0.5, -0.5, -0.5, -0.5).$$

Fig. 1 illustrates the identical synchronization error of the network described in (26). Specifically, in Fig. 1(a), we simulate the network without the controllers described in (27)-(29), with a coupling strength of $g_{syn} = 0.02$ over the time interval $t \in [0, 300000]$. The simulation indicates that the identical synchronization error does not converge to zero, implying that identical synchronization does not occur, even when t is extended to a large value.

Additionally, Fig. 2 presents the time series of all variables in the system described by (26) without the controllers. In Fig. 2(a), the variable u_1 is represented by the solid line, while the dotted line corresponds to u_2 (and similarly for v_1 and v_2 in Fig. 2(b), and w_1 and w_2 in Fig. 2(c)). From this, we can observe that the solid lines do not replicate the behavior of the dotted lines. In other words, the identical synchronization phenomenon does not occur in this scenario.

In Fig. 1(b), we simulate the network described by equation (26) using controllers (27)-(29), with a coupling strength of $g_{syn} = 0.0001$ and over the time interval $t \in [0, 4000]$. The simulation results show that the synchronization error between the identical variables reaches zero in a finite amount of time, despite the small coupling strength and the limited duration. This indicates that as time approaches a finite limit, the following approximations hold true:

$$u_1(t) \approx u_2(t), \quad v_1(t) \approx v_2(t), \quad w_1(t) \approx w_2(t).$$

Fig. 3 illustrates the time series of all variables in the system defined by (26) with the controllers (27)-(29). In Fig. 3(a), the variable u_1 is represented by the solid line, while u_2 is shown as a dotted line. Similarly, in Fig. 3(b), v_1 is solid and v_2 is dotted, and in Fig. 3(c), w_1 is the solid line and w_2 is dotted. The corresponding solid lines clearly mirror the behavior of the dotted lines, demonstrating the occurrence of identical synchronization. This synchronization takes place within the finite time frame, specifically for $t < 4000$.

B. Example 2.

This example examines a network comprising three linearly coupled nodes, as depicted in Fig. 4. The objective is to design a controller, grounded in the established theoretical framework, to achieve finite-time identical synchronization. Controllers for this network are developed based on the theoretical formulations presented in equations (8) through (10). The effectiveness of these controllers is subsequently evaluated via numerical simulations. The network topology and the associated control laws aimed at facilitating identical synchronization are defined by the following system:

$$\begin{cases} u_{1t} = f(u_1) + v_1 - w_1 + I, \\ v_{1t} = 1 - bu_1^2 - v_1, \\ w_{1t} = r(s(u_1 - c) - w_1), \\ u_{2t} = f(u_2) + v_2 - w_2 + I - g_{syn}(u_2 - u_1) + \Gamma_2^1, \\ v_{2t} = 1 - bu_2^2 - v_2 + \Gamma_2^2, \\ w_{2t} = r(s(u_2 - c) - w_2) + \Gamma_2^3, \\ u_{3t} = f(u_3) + v_3 - w_3 + I - g_{syn}(u_3 - u_1) + \Gamma_3^1, \\ v_{3t} = 1 - bu_3^2 - v_3 + \Gamma_3^2, \\ w_{3t} = r(s(u_3 - c) - w_3) + \Gamma_3^3. \end{cases} \tag{30}$$

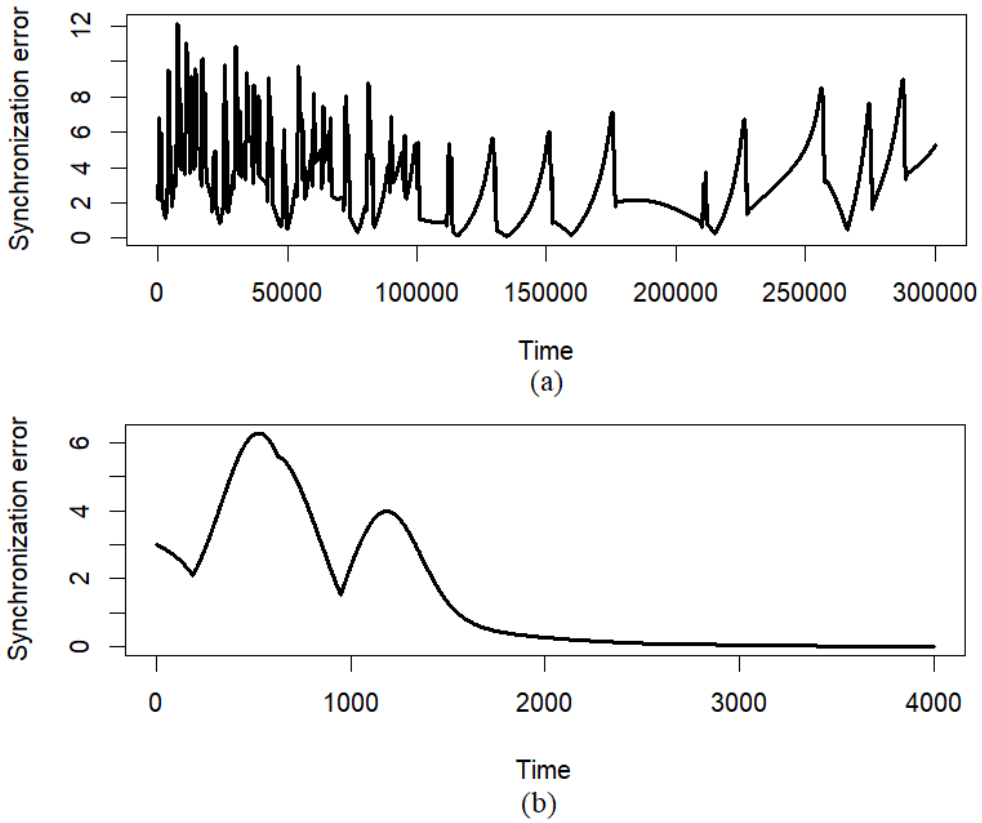

Fig. 1. Identical synchronization errors of the network (26): (a) without controllers (27)-(29); (b) with controllers (27)-(29).

where

$$\begin{cases} \Gamma_2^1 = u_{1t} - f(u_1) - v_1 + w_1 - I - k_2 e_2^u + G_2^1, \\ \Gamma_2^2 = v_{1t} - 1 + bu_1^2 + v_1 + G_2^2, \\ \Gamma_2^3 = w_{1t} - r(s(u_1 - c) - w_1) + G_2^3, \\ \Gamma_3^1 = u_{1t} - f(u_1) - v_1 + w_1 - I - k_3 e_3^u + G_3^1, \\ \Gamma_3^2 = v_{1t} - 1 + bu_1^2 + v_1 + G_3^2, \\ \Gamma_3^3 = w_{1t} - r(s(u_1 - c) - w_1) + G_3^3, \end{cases} \tag{31}$$

with the updated rules defined as follows:

$$\begin{cases} k_{2t} = r_2((e_2^u)^2 + \theta_2), \\ k_{3t} = r_3((e_3^u)^2 + \theta_3), \end{cases} \tag{32}$$

where $k_2 = k_2(t), k_3 = k_3(t)$; r_2, r_3 are arbitrary positive constants; $e_i^u = u_i - u_1, e_i^v = v_i - v_1, e_i^w = w_i - w_1, i = 2, 3$; and $G_i^j = G_i^j(t), \theta_i = \theta_i(t), i = 2, 3, j = 1, 2, 3$, are defined as follows:

$$\begin{cases} G_2^1 = -m.sign(e_2^u)|e_2^u|^\gamma, \\ G_2^2 = -m.sign(e_2^v)|e_2^v|^\gamma, \\ G_2^3 = -m.rs.sign(e_2^w)|e_2^w|^\gamma, \\ G_3^1 = -m.sign(e_3^u)|e_3^u|^\gamma, \\ G_3^2 = -m.sign(e_3^v)|e_3^v|^\gamma, \\ G_3^3 = -m.rs.sign(e_3^w)|e_3^w|^\gamma, \\ \theta_2 = -m.sign(k_2 - k).|k_2 - k|^\gamma, \\ \theta_3 = -m.sign(k_3 - k).|k_3 - k|^\gamma, \end{cases} \tag{33}$$

where $sign(.)$ represents a signum function, m is a given positive constant, $\gamma \in \mathbb{R}$ and satisfies $0 \leq \gamma < 1$.

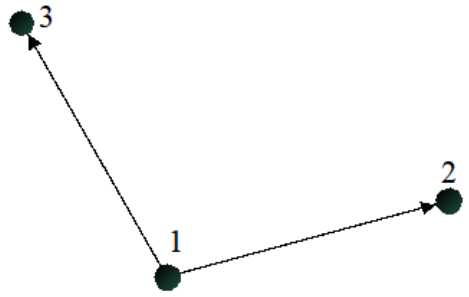

Fig. 4. A unidirectional graph consists of three nodes. The first node sends the signal to two other nodes and does not recieve any signal back from them.

In this example, we take:

$$m = 0.055;\ \gamma = 0.055; r_2 = 0.0002; r_3 = 0.002;$$

In addition, from (19), to ensure that the controller is effective, we need to choose the value of k large enough. Here, we take $k = 4$.

Let $|e_2^u|+|e_2^v|+|e_2^w|+|e_3^u|+|e_3^v|+|e_3^w|$ be the identical synchronization error. We say that the network (30) identically synchronizes in a finte time if the identical synchronization error reaches zero as t approaches a finite value. Here, we take the initial condition for the system (30) as follows:

$$(u_1(0), v_1(0), w_1(0)) = (1, 1, 1),$$
$$(u_2(0), v_2(0), w_2(0)) = (0.5, 0.5, 0.5),$$

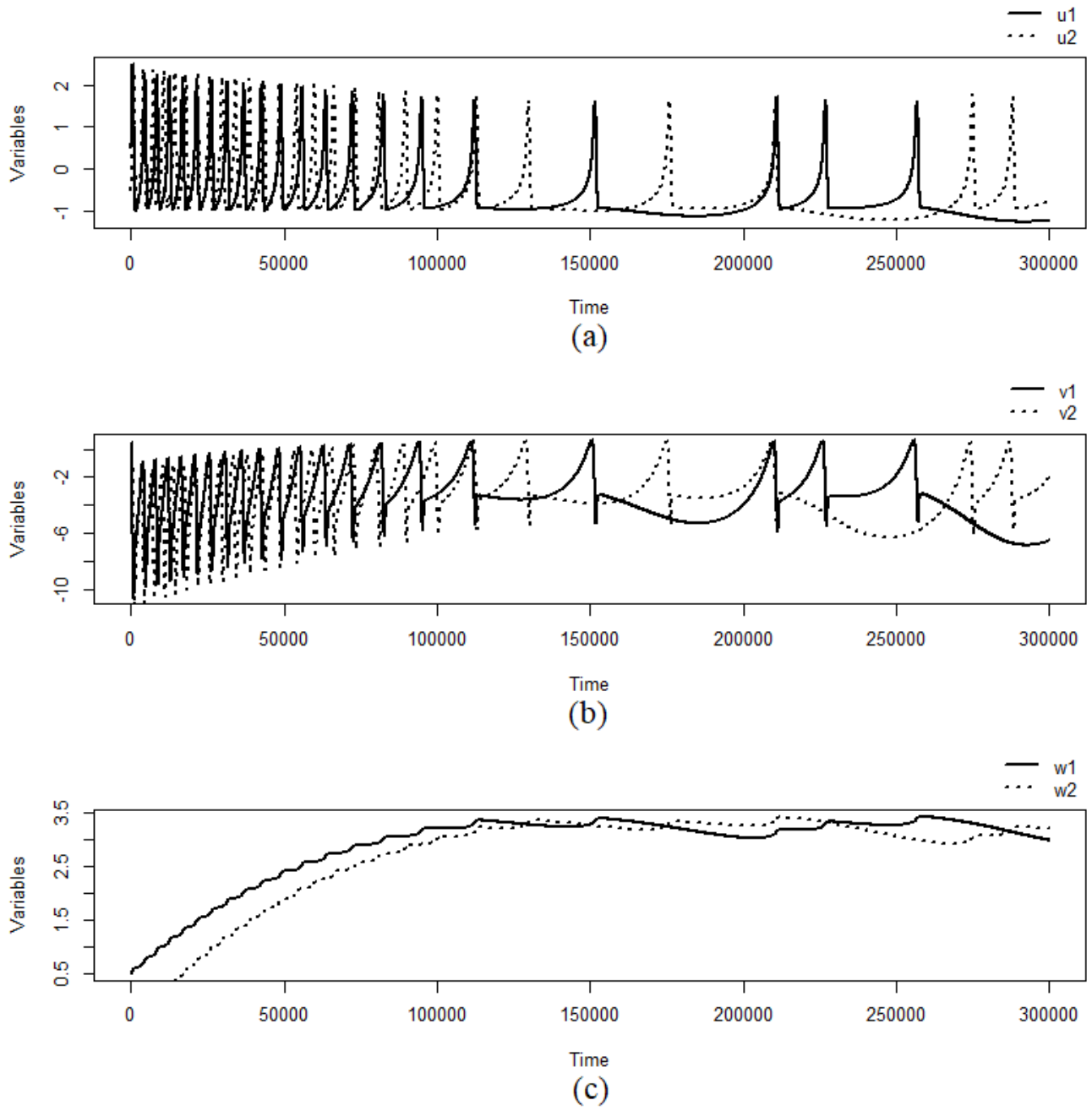

Fig. 2. Time series of all variables of the system (26) without controllers (27)-(29) accroding to the coupling strength $g_{syn} = 0.02$, and $t \in [0; 300000]$.

$$(u_3(0), v_3(0), w_3(0)) = (-1, -1, -1).$$

Fig. 5 illustrates the identical synchronization error of the network described by equation (30). In Fig. 5(a), we simulate the network without controllers (31)-(33) using a coupling strength of $g_{syn} = 0.9$ and for time $t \in [0, 200000]$. The simulation demonstrates that the identical synchronization error does not reach zero, indicating that the identical synchronization phenomenon does not occur, even when t is taken to be very large.

In Fig. 6, we present the time series of all variables of the system described by (30) without the aforementioned controllers. In Fig. 6(a), the variable u_1 is represented by the solid line, u_2 by the dotted line, and u_3 by the dashed line. Similarly, in Fig. 6(b), v_1, v_2, and v_3 are shown with solid, dotted, and dashed lines, respectively, while Fig. 6(c) shows w_1, w_2, and w_3 in the same manner. It is clear that the dotted and dashed lines do not replicate the behavior of the solid line, further confirming that the identical synchronization phenomenon does not occur in this scenario.

In contrast, Fig. 5(b) shows the simulation of the network with controllers (31)-(33), using a coupling strength of $g_{syn} = 0.5$ and for time $t \in [0, 100000]$. The results indicate that the identical synchronization error reaches zero in a finite time, even with a smaller coupling strength and shorter time t compared to the previous case. This suggests that as t approaches a finite value, we have the following approximations:

$$u_1(t) \approx u_2(t) \approx u_3(t);$$
$$v_1(t) \approx v_2(t) \approx v_3(t);$$
$$w_1(t) \approx w_2(t) \approx w_3(t.$$

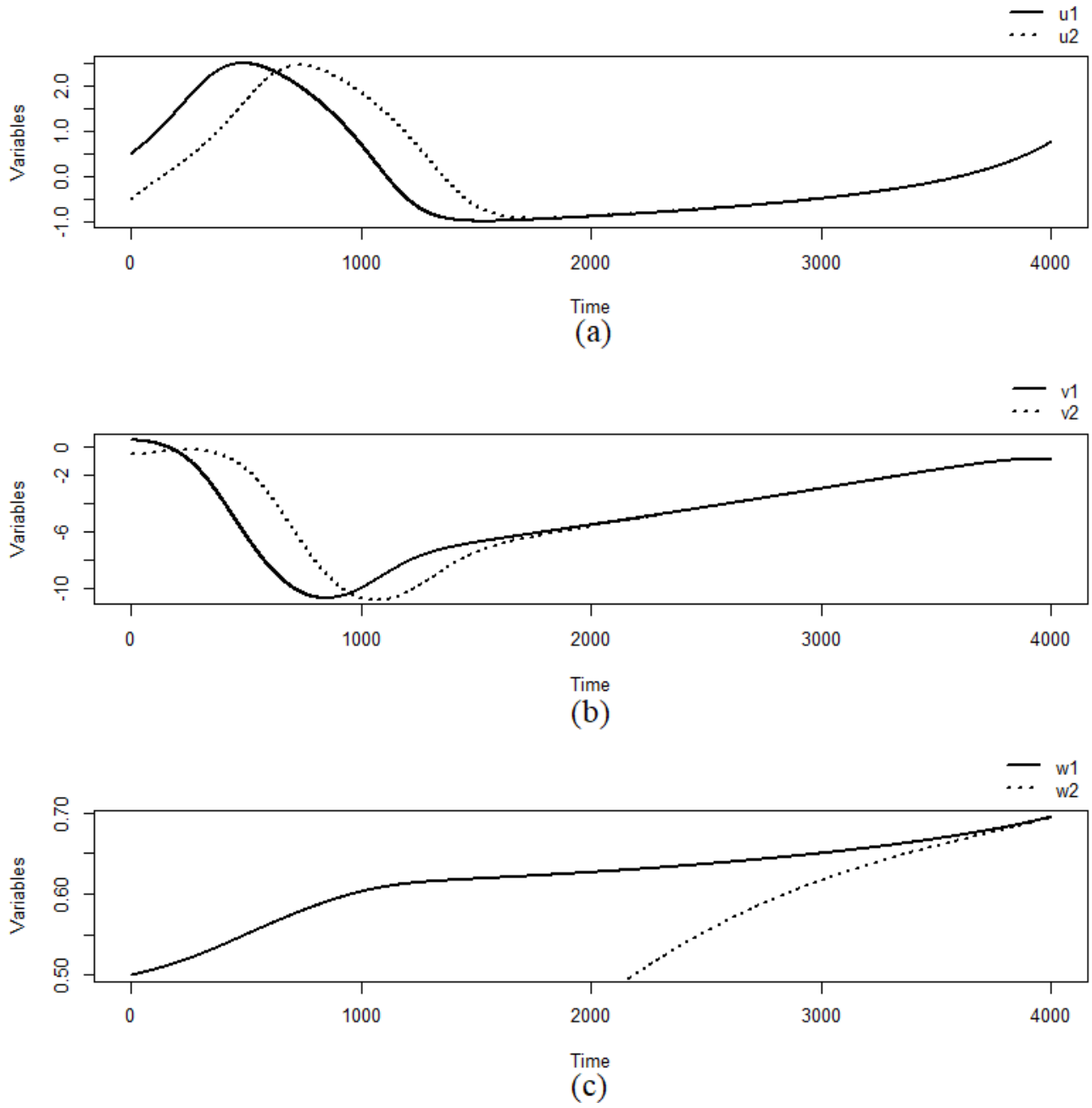

Fig. 3. Time series of all variables of the system (26) with controllers (27)-(29) according to the coupling strength $g_{syn} = 0.0001$, and $t \in [0; 4000]$.

Fig. 7 illustrates the time series of all variables in the system described by equations (30) and controlled by (31)-(33). In Fig. 7(a), the variable u_1 is represented by a solid line, while u_2 and u_3 are shown with dotted and dashed lines, respectively. Similarly, Fig. 7(b) displays v_1, v_2, and v_3 in the same line styles, and Fig. 7(c) shows w_1, w_2, and w_3. It is evident that the dotted and dashed lines closely replicate the behavior of the solid line. In other words, an identical synchronization phenomenon occurs in this case, and it happens within a finite time period (specifically, for $t < 90000$).

C. *Example 3.*

Consider a network composed of five linearly coupled nodes, as depicted in Fig. 8. The central aim is to develop a control strategy that guarantees finite-time identical synchronization across all nodes, building upon the theoretical constructs established in preceding sections. To achieve this objective, controllers are designed in accordance with the analytical framework presented in equations (8) through (10). These controllers incorporate coupling and control gains tailored to drive the network dynamics toward a synchronous manifold within a finite time interval. A critical aspect of this study involves validating the applicability and robustness of the proposed control laws under the networks inherent linear coupling structure. Specifically, we analyze the closed-loop system dynamics to confirm convergence properties and synchronization performance. The mathematical model governing the evolution of the coupled nodes, supplemented by the designed controllers, is formalized as follows. Through this formulation, the theoretical synchronization results are translated into a practical control scheme, facilitating both

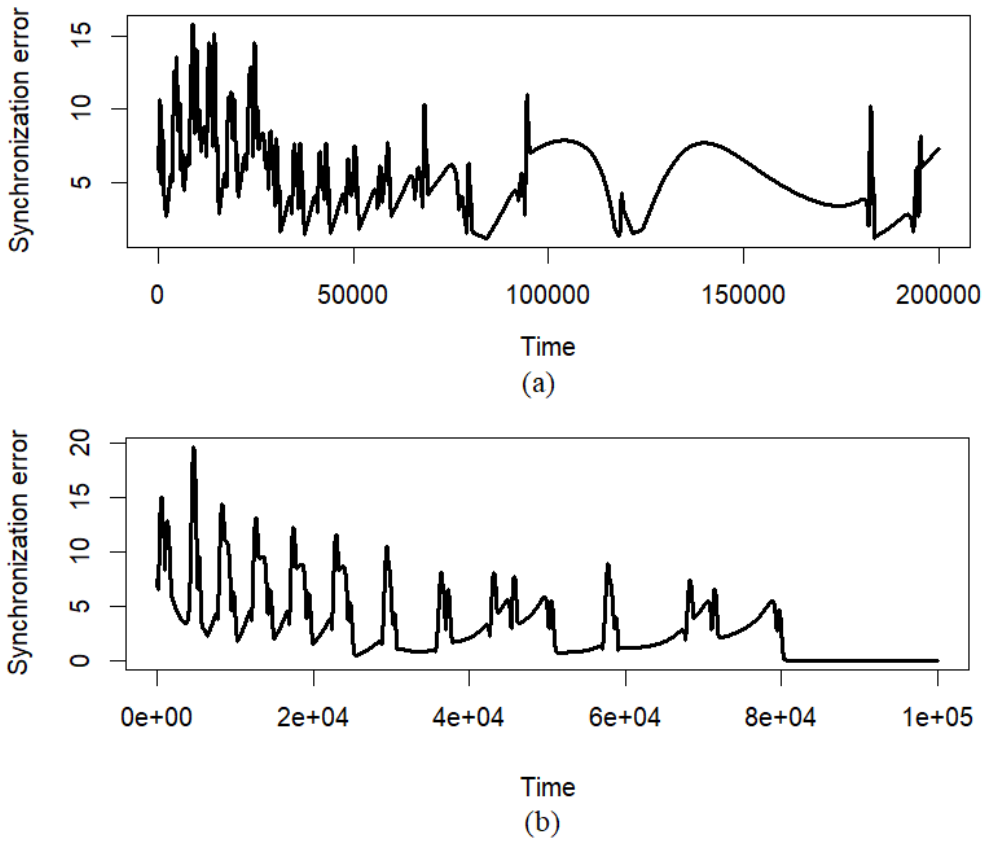

Fig. 5. Identical synchronization errors of the network (30): (a) without controllers (31)-(33); (b) with controllers (31)-(33).

numerical simulations and potential experimental implementations. This analysis not only substantiates the theoretical claims but also provides insights into controller design considerations for finite-time synchronization in complex coupled systems.

$$\begin{cases} u_{1t} = f(u_1) + v_1 - w_1 + I, \\ v_{1t} = 1 - bu_1^2 - v_1, \\ w_{1t} = r(s(u_1 - c) - w_1), \\ u_{2t} = f(u_2) + v_2 - w_2 + I - g_{syn}(u_2 - u_1) + \Gamma_2^1, \\ v_{2t} = 1 - bu_2^2 - v_2 + \Gamma_2^2, \\ w_{2t} = r(s(u_2 - c) - w_2) + \Gamma_2^3, \\ u_{3t} = f(u_3) + v_3 - w_3 + I - g_{syn}(u_3 - u_1) \\ \qquad\qquad -g_{syn}(u_3 - u_2) + \Gamma_3^1, \\ v_{3t} = 1 - bu_3^2 - v_3 + \Gamma_3^2, \\ w_{3t} = r(s(u_3 - c) - w_3) + \Gamma_3^3, \\ u_{4t} = f(u_4) + v_4 - w_4 + I - g_{syn}(u_4 - u_3) + \Gamma_4^1, \\ v_{4t} = 1 - bu_4^2 - v_4 + \Gamma_4^2, \\ w_{4t} = r(s(u_4 - c) - w_4) + \Gamma_4^3, \\ u_{5t} = f(u_5) + v_5 - w_5 + I - g_{syn}(u_5 - u_4) + \Gamma_5^1, \\ v_{5t} = 1 - bu_5^2 - v_5 + \Gamma_5^2, \\ w_{5t} = r(s(u_5 - c) - w_5) + \Gamma_5^3, \end{cases} \tag{34}$$

where

$$\begin{cases} \Gamma_2^1 = u_{1t} - f(u_1) - v_1 + w_1 - I - k_2 e_2^u + G_2^1, \\ \Gamma_2^2 = v_{1t} - 1 + bu_1^2 + v_1 + G_2^2, \\ \Gamma_2^3 = w_{1t} - r(s(u_1 - c) - w_1) + G_2^3, \\ \Gamma_3^1 = u_{1t} - f(u_1) - v_1 + w_1 - I \\ \qquad\qquad +g_{syn}(u_1 - u_2) - k_3 e_3^u + G_3^1, \\ \Gamma_3^2 = v_{1t} - 1 + bu_1^2 + v_1 + G_3^2, \\ \Gamma_3^3 = w_{1t} - r(s(u_1 - c) - w_1) + G_3^3, \\ \Gamma_4^1 = u_{1t} - f(u_1) - v_1 + w_1 - I \\ \qquad\qquad +g_{syn}(u_1 - u_3) - k_4 e_4^u + G_4^1, \\ \Gamma_4^2 = v_{1t} - 1 + bu_1^2 + v_1 + G_4^2, \\ \Gamma_4^3 = w_{1t} - r(s(u_1 - c) - w_1) + G_4^3, \\ \Gamma_5^1 = u_{1t} - f(u_1) - v_1 + w_1 - I \\ \qquad\qquad +g_{syn}(u_1 - u_4) - k_5 e_5^u + G_5^1, \\ \Gamma_5^2 = v_{1t} - 1 + bu_1^2 + v_1 + G_5^2, \\ \Gamma_5^3 = w_{1t} - r(s(u_1 - c) - w_1) + G_5^3, \end{cases} \tag{35}$$

with the updated rules defined as follows:

$$k_{it} = r_i((e_i^u)^2 + \theta_i),\ i = 2, 3, 4, 5, \tag{36}$$

where $k_i = k_i(t)$; r_i is an arbitrary positive constant; $e_i^u = u_i - u_1, e_i^v = v_i - v_1, e_i^w = w_i - w_1, i = 2, 3, 4, 5$; and $G_i^j = G_i^j(t), \theta_i = \theta_i(t), i = 2, 3, 4, 5, j = 1, 2, 3$, are defined as follows:

$$\begin{cases} G_i^1 = -m.sign(e_i^u)|e_i^u|^\gamma, \\ G_i^2 = -m.sign(e_i^v)|e_i^v|^\gamma, \\ G_i^3 = -m.rs.sign(e_i^w)|e_i^w|^\gamma, \end{cases} \tag{37}$$

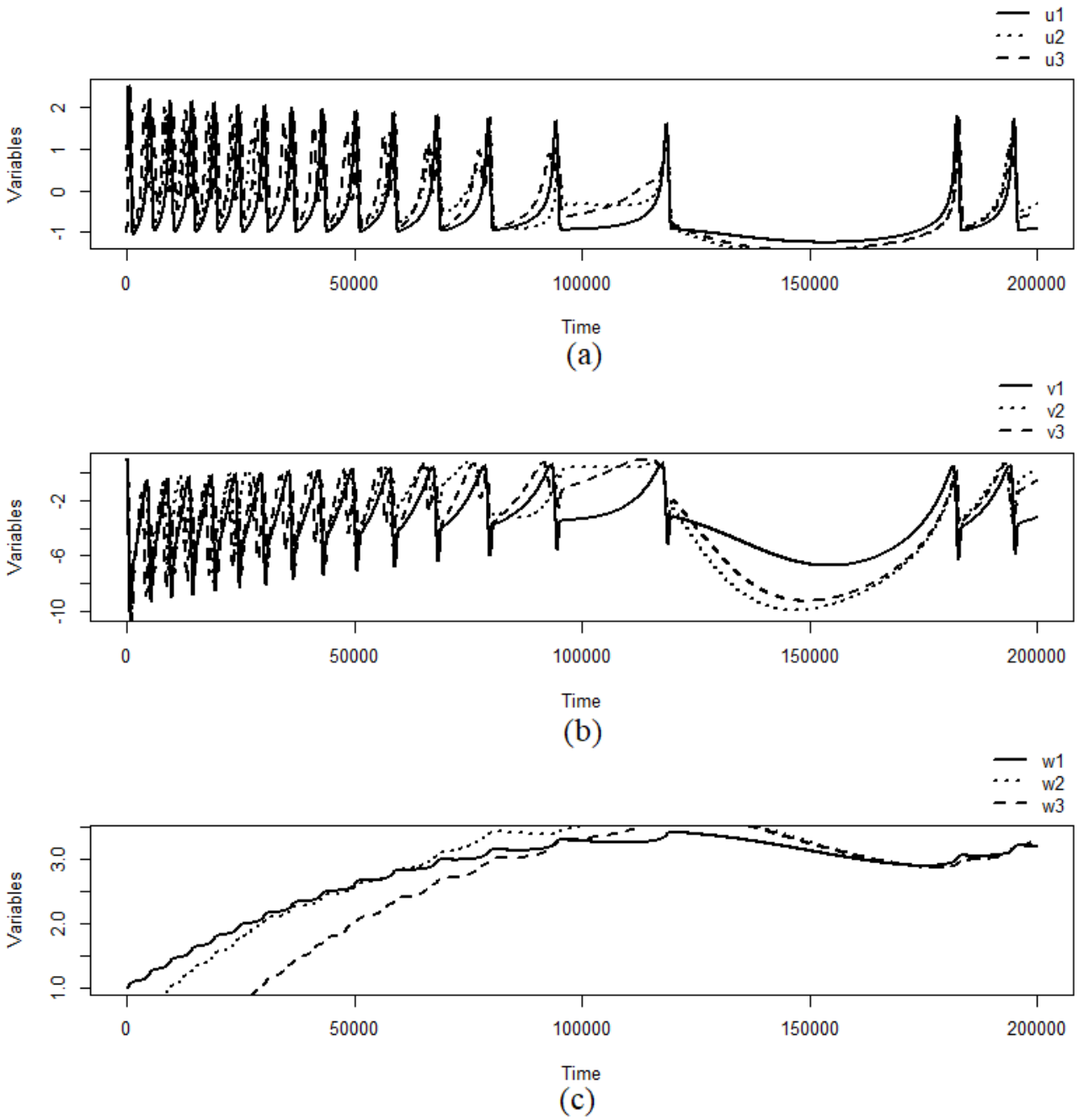

Fig. 6. Time series of all variables of the system (30) without controllers (31)-(33) accroding to the coupling strength $g_{syn} = 0.9$, and $t \in [0; 200000]$.

for all $i = 2, 3, 4, 5$, and

$$\theta_i = -m.sign(k_i - k).|k_i - k|^{\gamma},\ i = 2, 3, 4, 5, \qquad (38)$$

where $sign(.)$ represents a signum function, m is a given positive constant, $\gamma \in \mathbb{R}$ and satisfies $0 \leq \gamma < 1$.

In this example, we take:

$$m = 0.0055;\ \gamma = 0.0055;$$

$$r_2 = 0.0003; r_3 = 0.003; r_4 = 0.2; r_5 = 0.02.$$

In addition, from (19), to ensure that the controller is effective, we need to choose the value of k large enough. Here, we take $k = 4$.

Let $\sum_{i=2}^{5} |e_i^u| + |e_i^v| + |e_i^w|$ be the identical synchronization error. We say that the network (34) identically synchronizes in a finte time if the identical synchronization error reaches zero as t approaches a finite value. Here, we take the initial condition for the system (34) as follows:

$$(u_1(0), v_1(0), w_1(0)) = (1, 1, 1),$$
$$(u_2(0), v_2(0), w_2(0)) = (0.5, 0.5, 0.5),$$
$$(u_3(0), v_3(0), w_3(0)) = (-1, -1, -1),$$
$$(u_4(0), v_4(0), w_4(0)) = (0.5, 0.5, 0.5),$$
$$(u_5(0), v_5(0), w_5(0)) = (-1, -1, -1).$$

In this example, we set the coupling strength to a relatively high value to demonstrate that identical synchronization can occur even without a controller. However, it is important to

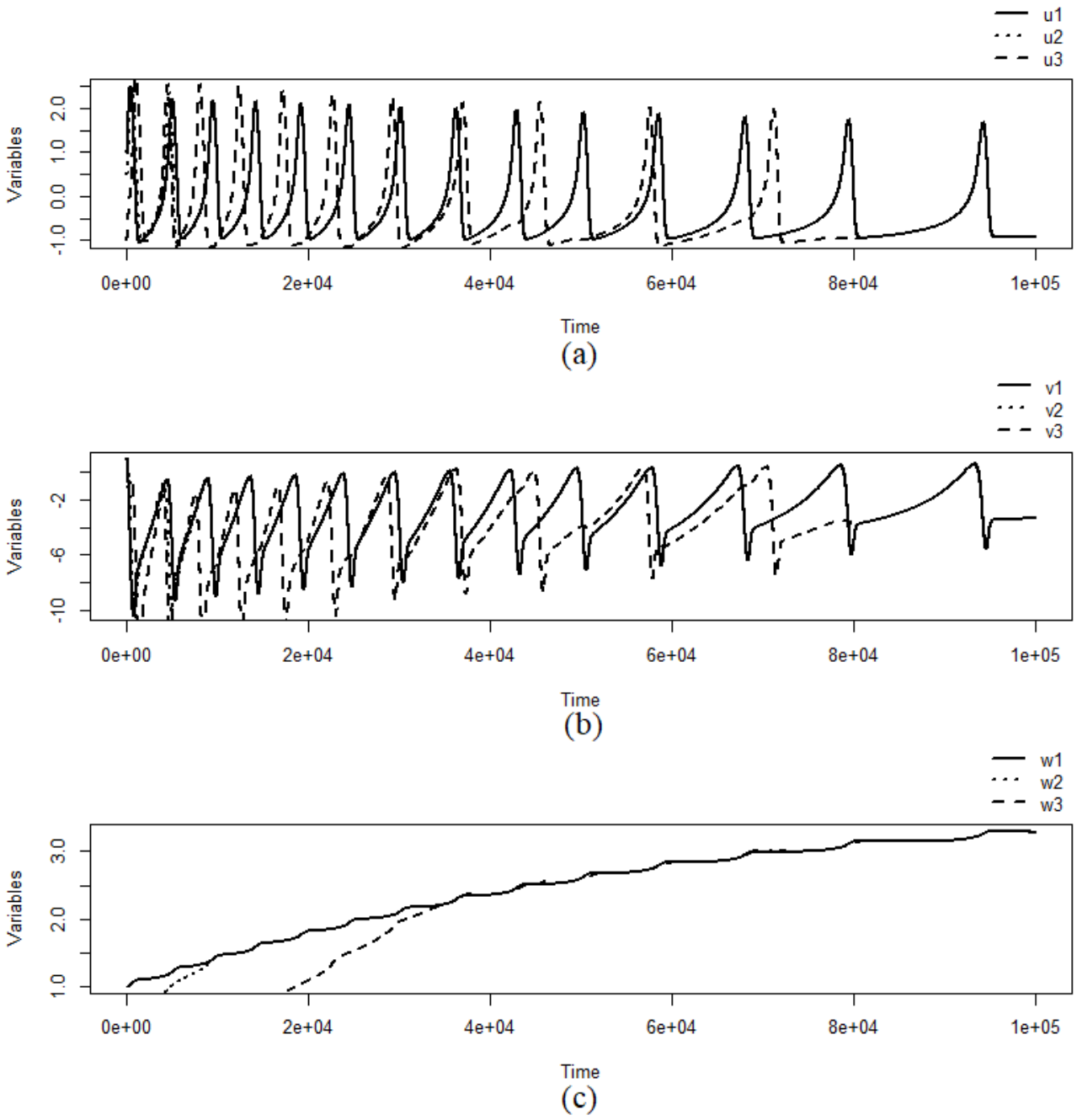

Fig. 7. Time series of all variables of the system (30) with controllers (31)-(33) according to the coupling strength $g_{syn} = 0.5$, and $t \in [0; 100000]$.

note that the time required to observe this phenomenon is quite extensive.

Fig. 9 illustrates the identical synchronization error of the network described in equation (34). Specifically, in Fig. 9(a), we simulate the network using equations (34) without the controllers outlined in equations (35)-(38), with a coupling strength of $g_{syn} = 1.2$ and for the time interval $t \in [0; 1000000]$. The simulation results show that the identical synchronization error reaches zero, indicating that identical synchronization occurs, albeit over a very long time period.

Conversely, in Fig. 9(b), we simulate the same network with the controllers specified in equations (35)-(38), again using the same coupling strength of $g_{syn} = 1.2$, but for the time interval $t \in [0; 150000]$. The results reveal that the identical synchronization error also reaches zero in this case. This indicates that identical synchronization occurs within a finite time frame ($t < 150000$).

Remark 4. The results obtained from the three numerical examples provide clear evidence of the effectiveness of the proposed control strategy in enhancing synchronization performance within linearly coupled dynamical networks. In Examples 1 and 2, synchronization is achieved in finite time by the controlled network, despite employing a smaller coupling strength than that used in the corresponding uncontrolled network. This illustrates that the introduction of the control input significantly improves convergence properties without necessitating stronger coupling between nodes. In Example 3, both controlled and uncontrolled networks are considered under a relatively large coupling strength. Although the uncontrolled network eventually reaches synchronization,

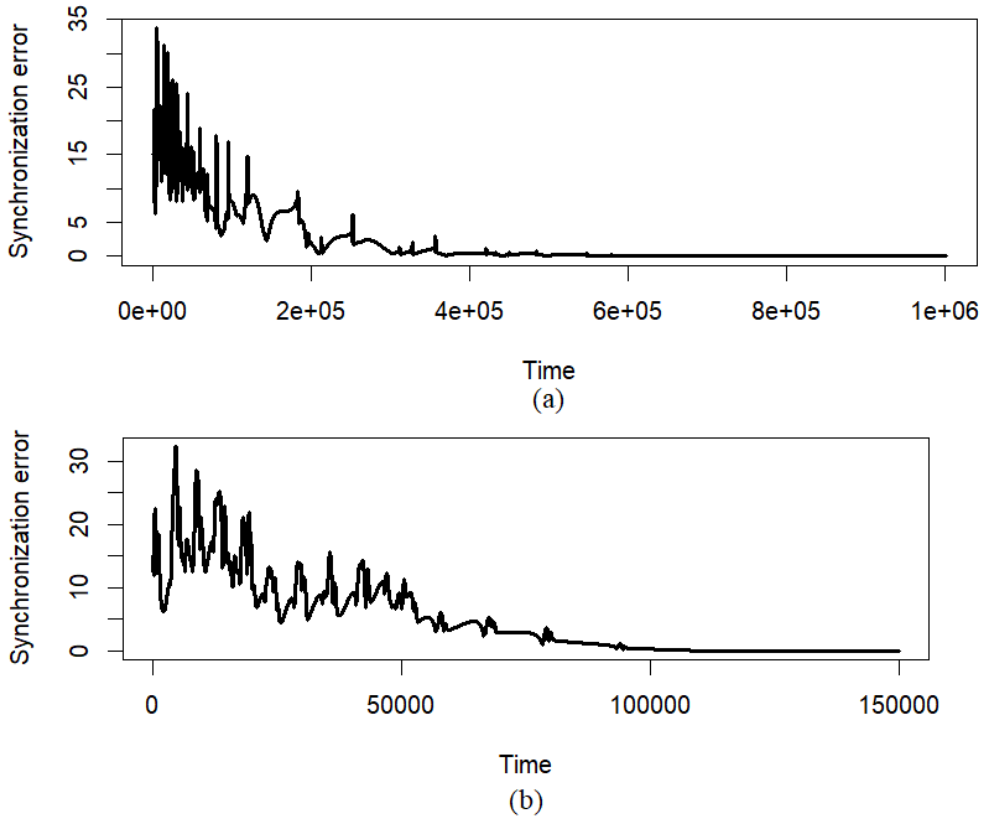

Fig. 9. Identical synchronization errors of the network (34): (a) without controllers (35)-(38); (b) with controllers (35)-(38).

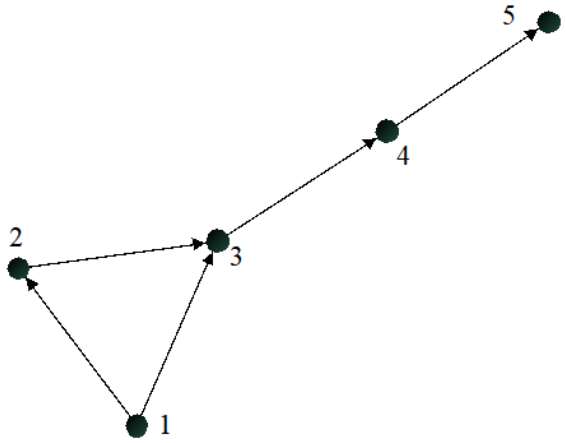

Fig. 8. A graph consists of five nodes with an arbitrary topological structure.

the time required is substantially longer compared to the controlled case. The network equipped with the proposed controller achieves identical synchronization within a considerably shorter time interval, further confirming the finite-time convergence guaranteed by the control design. These findings collectively demonstrate that the controller developed in this work not only accelerates the synchronization process but also reduces the dependence on coupling strength. As a result, the control strategy offers a practical and efficient mechanism for achieving finite-time synchronization in coupled dynamical systems, aligning with the theoretical framework established earlier in the study.

IV. Conclusion

This study investigates the problem of achieving identical synchronization in a network of n linearly coupled Hindmarsh-Rose 3D type dynamical systems, independent of the underlying network topology. A robust control strategy is developed based on finite-time stability theory and Lyapunov function methods. Sufficient conditions for finite-time synchronization are derived in the form of algebraic inequalities, providing a rigorous theoretical foundation for the proposed control scheme. The analysis guarantees that all nodes in the network converge to a common synchronous trajectory within a finite time interval. To validate the theoretical results, numerical simulations are conducted, demonstrating the controllers effectiveness and practical applicability. The findings confirm that the proposed method not only ensures synchronization under weaker coupling conditions but also significantly reduces convergence time. This work contributes a systematic and efficient framework for finite-time synchronization in complex networks of nonlinear dynamical systems.

References

[1] M. A. Aziz-Alaoui, "Synchronization of Chaos", *Encyclopedia of Mathematical Physics, Elsevier*, Vol. 5, pp. 213-226, 2006.
[2] N. Corson, "Dynamics of a neural model, synchronization and complexity", *Thesis, University of Le Havre*, France, 2009.
[3] A. Pikovsky, M. Rosenblum and J. Kurths, "Synchronization, A Universal Concept in Nonlinear Science", *Cambridge University Press*, 2001.
[4] A. L. Hodgkin and A. F. Huxley, "A quantitative description of membrane current and its application to conduction and excitation in nerve", *J. Physiol.117*, pp. 500-544, 1952.
[5] J. D. Murray, "Mathematical Biology", *Springer*, 2010.

[6] E. M. Izhikevich, "Dynamical Systems in Neuroscience", *The MIT Press*, 2007.

[7] G. B. Ermentrout and D. H. Terman, "Mathematical Foundations of Neurosciences", *Springer*, 2009.

[8] J. P. Keener and J. Sneyd, "Mathematical Physiology", *Springer*, 2009.

[9] J. L. Hindmarsh and R. M Rose, "A model of the nerve impulse using two firstorder differential equations", *Nature*, vol. 296, pp. 162-164, 1982.

[10] B. Ambrosio and M. A. Aziz-Alaoui, "Synchronization and control of coupled reaction-diffusion systems of the FitzHugh-Nagumo-type", *Computers and Mathematics with Applications*, vol 64, pp. 934-943, 2012.

[11] B. Ambrosio and M. A. Aziz-Alaoui, "Synchronization and control of a network of coupled reaction-diffusion systems of generalized FitzHugh-Nagumo type", *ESAIM: Proceedings*, Vol. 39, pp. 15-24, 2013.

[12] D. Aeyels, "Asymptotic Stability of Nonautonomous Systems by Lyapunov's Direct Method", *Systems and Control Letters,* 25, 273-280, 1995.

[13] I. Belykh, E. De Lange and M. Hasler, "Synchronization of bursting neurons: What matters in the network topology", *Phys. Rev. Lett.* 188101, 2005.

[14] V. L. E. Phan, "Sufficient Condition for Synchronization in Complete Networks of Reaction-Diffusion Equations of Hindmarsh-Rose Type with Linear Coupling", *IAENG International Journal of Applied Mathematics*, vol. 52, no. 2, pp. 315-319, 2022.

[15] V. L. E. Phan, "Sufficient Condition for Synchronization in Complete Networks of n Reaction-Diffusion Systems of Hindmarsh-Rose Type with Nonlinear Coupling", *Engineering Letters,*, vol. 31, no. 1, pp413-418, 2023.

[16] V. L. E. Phan, "Global Attractor of Networks of n Coupled Reaction-Diffusion Systems of Hindmarsh-Rose Type", *Engineering Letters,* vol. 31, no. 3, pp1215-1220, 2023.

[17] V. L. E. Phan, "Synchronous Controller between Drive Network of n Reaction-Diffusion Systems of FitzHugh - Nagumo type and Response Network of n Reaction-Diffusion Systems of Hindmarsh-Rose type", *IAENG International Journal of Applied Mathematics*, vol. 54, no. 10, pp2049-2059, 2024.

[18] D. W. Jordan and P. Smith, "Nonlinear Ordinary Differential Equations, An Introduction for Scientists and engineers (4th Edition)", *Oxford*, 2007.

[19] C.J. Qian and J. Li, *Global Finite-Time Stabilization by Output Feedback for Planar Systems without Observable Linearization,* IEEE Transactions on Automatic Control, **50**, 885-890. https://doi.org/10.1109/TAC.2005.849253, 2005.

[20] S.P. Bhat and D.S. Bernstein, *Finite-time Stability of Continuous Autonomous Systems,* SIAM Journal on Control and Optimization, **38**, 751-766. https://doi.org/10.1137/S0363012997321358, 2000.

[21] S. Stogatz and I. Stewart, "Coupled Oscillators and Biological Synchronization", *Scientific American,* 269, 102-109, 1993.

[22] S. H. Strogatz, "Exploring Complex Networks", *Nature,* 410, 268-276, 2001.

[23] Q. Xie, R.G. Chen and E. Bolt, "Hybrid Chaos Synchronization and Its Application in Information Processing", *Mathematical and Computer Modelling,* 1, 145-163, 2002.

[24] C.M. Gray, "Synchronous Oscillations in Neural Systems", *Journal of Computational Neuroscience,* 1, 11-38, 1994.